BIOCHEMISTRY
including biophysical chemistry & molecular biology
Article

Biochemistry **2010,** *49,* 5511–5523 5511
DOI: 10.1021/bi100157u

Membrane Localization of LRRK2 Is Associated with Increased Formation of the Highly Active LRRK2 Dimer and Changes in Its Phosphorylation†

Zdenek Berger,[‡,§] Kelsey A. Smith,[‡] and Matthew J. LaVoie*[,‡,§]

[‡]*Center for Neurologic Diseases, Department of Neurology, Brigham and Women's Hospital, Boston, Massachusetts 02115, and* [§]*Harvard Medical School, Boston, Massachusetts 02115*

Received February 1, 2010; Revised Manuscript Received May 29, 2010

ABSTRACT: Autosomal dominant mutations in leucine rich repeat kinase 2 (LRRK2) are the most common genetic cause of Parkinson's disease (PD). Despite the presence of multiple domains, the kinase activity of LRRK2 is thought to represent the primary function of the protein. Alterations in LRRK2 kinase activity are thought to underlie the pathogenesis of its PD-linked mutations; however, many questions regarding basic aspects of LRRK2 function remain unclear, including the cellular mechanisms of LRRK2 regulation and the importance of its unique distribution within the cell. Here, we demonstrate for the first time that the subcellular localization of wild-type LRRK2 is associated with changes in four distinct biochemical properties likely crucial for LRRK2 function. Our data demonstrate for the first time that the wild-type LRRK2 dimer possesses greater kinase activity than its more abundant monomeric counterpart. Importantly, we show that this activated form of LRRK2 is substantially enriched at the membrane of cells expressing endogenous or exogenous LRRK2, and that the membrane-associated fraction of LRRK2 likewise possesses greater kinase activity than cytosolic LRRK2. In addition, membrane-associated LRRK2 binds GTP more efficiently than cytosolic LRRK2 but demonstrates a lower degree of phosphorylation. Our observations suggest that multiple events, including altered protein−protein interactions and post-translational modifications, contribute to the regulation of LRRK2 function, through modulation of membrane association and complex assembly. These findings may have implications for the sites of LRRK2 function within the cell, the identification and localization of bona fide LRRK2 substrates, and efforts to design small molecule inhibitors of LRRK2.

Parkinson's disease (PD)[1] is the second most common neurodegenerative disorder, affecting ~2% of the population over the age of 50, with ~1.5 million patients in the United States alone (*1*). Mutations in multiple genes are now known to cause familial PD (*2*, *3*), paving the way for molecular approaches to studying the disease. The most common mutations in PD are found in leucine rich repeat kinase 2 (LRRK2). They account for between 5 and 40% of familial parkinsonism and for 0.5−2.0% of sporadic PD cases (*2*, *4*−*6*). The vast majority of cases with LRRK2 mutations present pathologically with α-synuclein inclusions, as in classic idiopathic PD (*4*, *6*), establishing the likelihood that studying LRRK2 may shed light on the pathogenic mechanisms underlying all PD cases. Although mutations in LRRK2 demonstrate an autosomal dominant inheritance pattern, their penetrance is age-dependent and incomplete (*7*−*10*). These observations suggest the existence of regulatory pathways that control LRRK2 activity, as is true for most kinases. However, little is known about how cells might regulate LRRK2 activity and what biochemical events would be responsible.

LRRK2 encodes a large protein of 2527 amino acids with PD-linked mutations spanning the entire protein, including its kinase and Roc (GTPase) domains (*5*, *6*, *11*). The kinase domain is homologous to other MAPKKKs, and its activity is believed to be crucial for its function and may also be important for the pathogenic processes in PD (*12*−*20*). Immunohistochemical and electron microscopic analyses of LRRK2 revealed the presence of the protein in the proximity of numerous membrane structures in mammalian brain (*21*), and biochemical studies have validated the membrane association of LRRK2 (*22*). Interestingly, LRRK2 has been implicated in diverse cellular processes, most of which either involve membrane dynamics or occur at the membrane, such as maintenance of neurite morphology (*23*, *24*), vesicle endocytosis (*25*), autophagy (*24*, *26*), and Wnt signaling (*27*). However, the importance of this subcellular localization on the biochemical properties of LRRK2 or its function has not been previously examined.

LRRK2 recently has been suggested to form a dimer (*28*−*30*) in intact cells. Furthermore, an in vitro study using a recombinant ROC domain fragment of LRRK2 indicated that the R1441C mutation destabilizes the LRRK2 dimer (*31*), implying a potential role for altered dimerization of LRRK2 in PD pathogenesis. However, there are several outstanding questions to be addressed with regard to the LRRK2 dimer, including the respective activity of monomeric and dimeric LRRK2 and whether the LRRK2 dimer possesses a specialized distribution within the cell.

Although LRRK2 is present both in the cytosol and at the membrane (*21*, *22*), it is not known whether the presence of

†This work was supported by an Edward R. and Anne G. Lefler Postdoctoral Fellowship (Z.B.), National Institutes of Health Grant AG023094 (M.J.L.), and the Brigham and Women's Hospital Udall Center of Excellence for Parkinson's Disease Research (NS038375).

*To whom correspondence should be addressed. E-mail: mlavoie@rics.bwh.harvard.edu. Phone: (617) 525-5185. Fax: (617) 525-5252.

[1]Abbreviations: KD, kinase dead; LMW, low-molecular weight; LRRK2, leucine rich repeat kinase; MBP, myelin basic protein; IP, immunoprecipitation; GDP, guanosine diphosphate; GTP, guanosine triphosphate; HMW, high-molecular weight; PD, Parkinson's disease.

Published on Web 06/01/2010

LRRK2 in different subcellular compartments is associated with meaningful consequences for LRRK2 function or activity. In this study, we show that the LRRK2 dimer is substantially enriched at the membrane, which coincides with greater in vitro kinase activity of the membrane-associated pool of LRRK2 compared to cytosolic LRRK2. We also demonstrate that the less abundant LRRK2 dimer is more active (per molecule) than the more abundant LRRK2 monomer. We have established further biochemical distinctions between membrane-bound and cytosolic LRRK2. Membrane-associated LRRK2 studied from multiple systems was found to bind GTP more efficiently and was also found to be phosphorylated to a lesser extent than cytosolic LRRK2. Our data suggest that subcellular localization of LRRK2 is important for its activity, complex formation, and function, and that the membrane-associated LRRK2 dimer may represent the physiologically active form of the protein.

MATERIALS AND METHODS

Cell Culture. GFP-LRRK2 and myc-LRRK2 constructs containing the entire ORF of LRRK2 (generous gifts of M. Cookson) were transiently transfected into HEK293FT cells (Invitrogen) using Lipofectamine 2000 (Invitrogen) according to the manufacturer's instructions. Cells were harvested in ice-cold PBS approximately 24 h after transfection. HEK293FT cells were cultured in Dulbecco's modified Eagle's medium (DMEM), 10% fetal bovine serum, 100 units/mL penicillin, 0.1 mg/mL streptomycin, 0.5 mg/mL geneticin, 2 mM L-glutamine, 0.1 mM MEM nonessential amino acids, and 1 mM MEM sodium pyruvate. Lymphoblasts (Coriell ID ND06358) were cultured in RPMI 1640, 2 mM L-glutamine, 100 units/mL penicillin, 0.1 mg/mL streptomycin, and 15% fetal bovine serum. The rodent midbrain dopaminergic MES23.5 (MES) cells were cultured as previously described (*32*).

Generation of Cytosol and Membrane Fractions. Cells were mechanically disrupted in lysis buffer [50 mM HEPES, 150 mM NaCl, PMSF, protease inhibitors, and phosphatase inhibitors I and II (Sigma), 2 mM EDTA, 2 mM EGTA, 10 mM $Na_4P_2O_7 \cdot 10H_2O$, 20 mM NaF, 2 mM Na_3VO_4 (Sigma)] by using 20 gentle strokes of a Potter-Elvehjem homogenizer. The resulting homogenate was then drawn with an 18.5 gauge needle and expelled through a 27.5 gauge needle five times. Homogenates were subsequently centrifuged at 1000*g* for 10 min; the pellet was discarded, and the supernatant was further centrifuged at 100000*g* for 1 h. The 100000*g* supernatant was used as the cytosol, while the 100000*g* pellet represented the membrane fraction. For Western blot analysis, this 100000*g* pellet was resuspended in 2× Laemmli buffer and sonicated. For all other analyses (e.g., in vitro kinase assay and chemical cross-linking), the 100000*g* pellet was first extracted for 30 min on ice using the same lysis buffer supplemented with Triton X-100 (Sigma) to a final concentration of 1%, unless mentioned otherwise, and then centrifuged at 10000*g* for 10 min. The Triton-soluble supernatant constituted the membrane fraction. Following fractionation, and prior to separation with a glycerol velocity gradient (see below), Triton X-100 was supplemented to the cytosol samples to the same final concentration as the membrane fractions.

Glycerol Velocity Gradients. Whole-cell extracts for glycerol velocity gradients were prepared by lysing cells on ice for 30 min in 0.5% Triton X-100, 50 mM HEPES (pH 7.4), 150 mM NaCl, PMSF, protease inhibitors (Sigma), phosphatase inhibitors I and II (Sigma), 2 mM EDTA, 2 mM EGTA, 10 mM $Na_4P_2O_7 \cdot 10H_2O$, 20 mM NaF, 2 mM Na_3VO_4 (Sigma), and 2 mM DTT. The lysates were subsequently centrifuged at 10000*g* for 10 min, and the supernatant was used for further analysis. Comparison between centrifugation of the sample at 10000*g* for 10 min and 100000*g* for 1 h revealed no differences in LRRK2 distribution across the gradient (not shown). Cytosol and membrane fractions were prepared as described above; a final concentration of 0.5% Triton X-100 was used in both cytosol and membrane fractions. Addition of 0.5% Triton X-100 to the cytosol revealed no differences in LRRK2 distribution across the gradient (not shown). Glycerol gradients were prepared in 25 mM HEPES (pH 7.4), 0.5% Triton X-100, and 1 mM DTT. Samples were layered on top of the glycerol gradient and centrifuged at 100000*g* for 16 h at 4 °C. Equal volumes of each glycerol fraction were analyzed by Western blot. For quantifications of the relative amount of LMW and HMW LRRK2, the boundary between these fractions was defined as the fraction with the lowest intensity and fractions with the lower molecular weight (typically 15−21% glycerol) were considered as LMW and fractions corresponding to the higher molecular weight (typically 25−35% glycerol) HMW LRRK2. Glycerol gradients were calibrated using commercially available standards of known molecular weights: BSA (67000), LDH (140000), catalase (232000), ferritin (440000) (GE Healthcare), and urease (Sigma) which occurs natively as a trimer and hexamer with molecular weights of 272000 and 545000, respectively. The distribution of LRRK2 across the glycerol gradients was verified in at least three independent experiments for each condition. To determine which glycerol fractions contained γ secretase complex and mitochondrial complex I subunit, cells were lysed in 1% CHAPS (to retain the native assembly state for both protein complexes) and subsequently analyzed using glycerol gradients containing 1% CHAPS.

Heterologous Co-Immunoprecipitation (*co-IP*). The expression levels of myc-LRRK2 were matched to the expression levels of GFP-LRRK2 in an independent experiment by titrating the amount of myc-LRRK2 cDNA used during transfection (for each set of plasmid DNA). The amount of DNA per transfection was kept constant by using an empty vector (pcDNA 3.1). Cell lysates were protein normalized and analyzed by Western blot using an anti-LRRK2 antibody (see below). Cytosol and membrane fractions in 0.1% Triton X-100 were immunoprecipitated (IPed) using agarose-conjugated anti-c-myc resin (Vector Laboratories), followed by five washes using lysis buffer supplemented with 0.1% Triton X-100. The resin was heated to 65 °C in 2× Laemmli buffer with β-mercaptoethanol for 5−10 min, and samples were analyzed by Western blot. In each experiment, cells transfected with GFP-LRRK2 and empty vector were used as a control for nonspecific binding of GFP-LRRK2 to the myc resin. Three independent experiments were performed to quantify relative LRRK2 dimer levels.

In Vitro Kinase Assays. LRRK2 was IPed using anti-c-myc agarose affinity resin (Sigma, catalog no. A7470), followed by two washes in lysis buffer with 500 mM NaCl, three washes with lysis buffer (150 mM NaCl), one with lysis buffer with no detergent, and one with kinase buffer (see below) without ATP. Kinase reactions were performed in 25 mM Tris (pH 7.5), 5 mM β-glycerophosphate, 0.1 mM sodium vanadate, 10 mM magnesium chloride, 50 μM cold ATP, and 10 μCi of [γ-^{32}P]ATP for 30 min at 30 °C. The reaction was stopped via addition of 4× Laemmli buffer with β-mercaptoethanol. A small aliquot was analyzed by Western blot using the Odyssey infrared imaging system (LI-COR Biosciences). The remainder of the

reaction mixture was loaded onto 6% Tris-glycine gels (Invitrogen), dried, and exposed to autoradiography film (Kodak). LRRK2 kinase activity was quantified by measuring the intensity of [^{32}P]LRRK2 on the autoradiograph and normalizing it to the amount of LRRK2 protein by Western blot. Three independent experiments were performed to determine the relative activities of cytosolic and membrane-associated LRRK2. Detailed experiments revealed that the occasional doublet pattern of LRRK2 on SDS−PAGE indeed represents two bands both corresponding to full-length LRRK2. Therefore, both bands were considered for quantitative analysis, if present. The presence of the doublet did not correlate with any specific condition and was observed in both membrane and cytosol fractions.

For in vitro kinase assays from the glycerol gradients, the distribution of LRRK2 across each glycerol gradient was first verified by Western blot, and LMW (15−19%) and HMW (25−35%) fractions from multiple gradients were then pooled and used for myc IP. Six independent experiments were conducted to assess the relative activities of LMW and HMW LRRK2. To ensure optimal IP conditions, we then diluted each fraction to a final concentration of 10% glycerol and concentrated each using Amicon Ultra centrifuge devices with a 100000 cutoff. We did not observe any loss of LRRK2 following concentration, indicating no appreciable binding of LRRK2 to the filter. Of note, we observed similar results (increased kinase activity from HMW vs LMW LRRK2) without concentrating the samples, ruling out artifacts from the concentration procedure itself.

Chemical Cross-Linking. Live cells were cross-linked with DSS, DST, SATP, BMOE, or BMH (Pierce) at room temperature for 30 min in PBS with 10 mM EDTA, according to the manufacturer's instructions. Control samples were incubated with the vehicle (DMSO) at the same time. Cytosol and membrane fractions (final concentration of 1% Triton X-100) were protein normalized prior to cross-linking, with equal volumes used. Each experiment was repeated three times. For cross-linking of glycerol gradient fractions, 15 and 29% glycerol fractions were used as the LMW and HMW forms, respectively.

Western Blot. Samples were mixed with 4× Laemmli buffer with 20% β-mercaptoethanol, heated at 65 °C for 5 min, and loaded onto Novex (Invitrogen) or Criterion (Bio-Rad) Tris-Glycine precast gels. The proteins were subsequently transferred onto polyvinylidene fluoride (PVDF) membranes (Millipore) and probed with the anti-myc antibody (polyclonal A14 or monoclonal 9E10, 1:1000 or 1:500, respectively; Santa Cruz Biotechnology), anti-LRRK2 (custom affinity-purified polyclonal LRRK2 antibody raised against the C-terminus, antigen sequence of EKHIEVRKELAEKMRRTSVE), monoclonal anti-actin (1:50000; Sigma), or the monoclonal anti-transferrin receptor (1:1000; Zymed), monoclonal anti-GAPDH (1:20000; Chemicon), monoclonal anti-NDUFA9 (1:1000; Mitosciences), polyclonal anti-nicastrin (1:1000; Sigma, N1660), and polyclonal presenilin 1 NTF (1:1000; Calbiochem). Secondary antibodies (1:2000 to 1:10000) and ECL-plus were purchased from GE Healthcare. Following ECL application, blots were exposed to HyBlot Cl autoradiography film (Metuchen). Densitometry was conducted using AlphaEase Automatic Image Capture (Alpha Innotech). Some Western blots were developed using the Odyssey infrared imaging system (LI-COR Biosciences), including those used to quantify LRRK2 levels from in vitro kinase reactions. The Odyssey system was used in conjunction with an infrared anti-mouse secondary antibody (1:5000, Rockland Immunochemicals).

Phosphoprotein Analyses. Cytosolic and membrane fractions were prepared and IPed using the high-affinity anti-c-myc agarose resin (Sigma, catalog no. A7470), as described above for in vitro kinase assays. Samples were separated by SDS−PAGE and the gels then fixed and stained with Pro-Q Diamond Phosphoprotein gel stain (Invitrogen), according to the manufacturer's instructions. The gel was visualized using FLA-9000 (FujiFilm, excitation at 532 nm, LPG filter). Subsequently, the same gel was stained for total proteins using SYPRO Ruby (Invitrogen) and visualized either using FLA-9000 (FujiFilm, excitation at 473 nm, LPG filter) or a UV transilluminator (Alpha Innotech). The relative levels of LRRK2 phosphorylation were quantified by normalization of the intensity of the phosphoprotein signal to the levels of total LRRK2 (SYPRO Ruby stain or Western blot). Cytosolic and membrane fractions of both untransfected cells and myc-LRRK2-transfected cells were analyzed in parallel. Three independent experiments were performed to quantify the relative phospho-LRRK2 levels in the cytosolic and membrane fractions.

GTP Binding. GTP binding was performed as previously described (*33*−*35*) with minor modifications. Samples were prepared as described above, and the cytosolic fraction was supplemented with Triton X-100 to a final concentration of 1%, to match the buffer conditions of the corresponding membrane fraction. The volume of all samples was kept constant within a given experiment, and we ensured that the protein levels remained below the saturating capacity of the GTP resin. Prior to GTP binding, the GTP-agarose resin was blocked with 100 μg/mL BSA in PBS for 1 h. Cell lysates were incubated for 1 h at 4 °C, followed by three washes in lysis buffer with 1% Triton X-100, and then specifically bound LRRK2 was eluted with 2 mM GTP for 90 min. Three independent experiments were performed using both cytosol and membrane fractions.

Size Exclusion Chromatography. Size exclusion chromatography was conducted at 4 °C using an AKTA-FPLC system (GE Healthcare). Samples were injected onto a Superdex 200 10/300 GL column (GE Healthcare) equilibrated in 50 mM HEPES (pH 7.4) and 150 mM NaCl (unless mentioned otherwise) and eluted using the same buffer at a flow rate of 0.2 mL/min. Fractions (0.25 mL) were analyzed by Western blot, as described above. The column was calibrated using the following standards and corresponding elution volumes: thyroglobulin (669000, 9.5 mL; Bio-Rad), apoferritin (440000, 11.32 mL; Sigma), catalase (232000, 12.97 mL; Sigma), aldolase (158000, 13.37 mL; GE Healthcare), conalbumin (75000, 14.67 mL; GE Healthcare), ovalbumin (44000, 15.63 mL; Bio-Rad), and myoglobin (17000, 17.59 mL; Bio-Rad). Blue dextran was used to confirm the void volume (8.79 mL; GE Healthcare).

Blue-Native PAGE. Blue-Native PAGE was performed according to the manufacturer's instructions (Invitrogen) using 3 to 12% Bis-Tris native gels. After electrophoresis, the gel was incubated in transfer buffer containing 0.1% SDS for 10−15 min and subsequently transferred to PVDF in the presence of 0.01% SDS to improve the transfer efficiency of HMW protein complexes. Two independent molecular weight standards were purchased from GE Healthcare and Invitrogen. To determine the relative migration of LRRK2, these standards were run on adjacent lanes along with LRRK2 samples and analyzed both on the gel itself (Coomassie staining) and on the membrane (after transfer on the PVDF membrane and staining with Ponceau S).

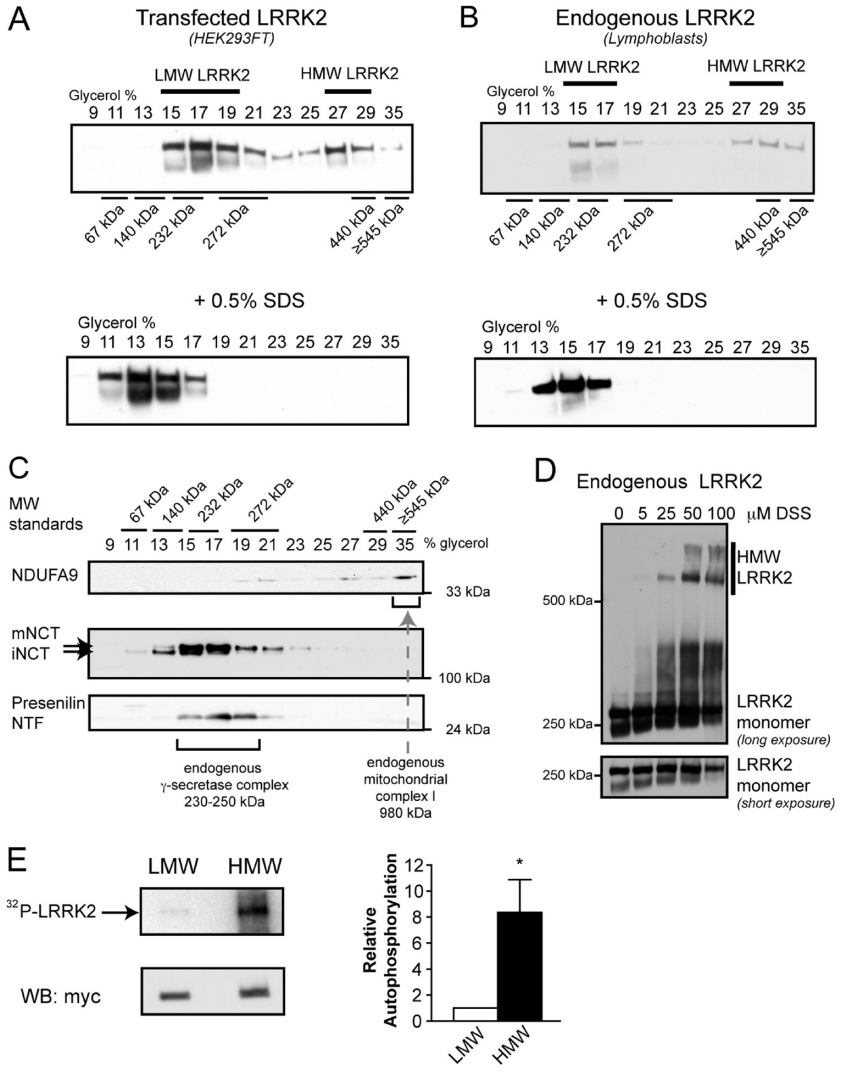

FIGURE 1: Analysis of HMW and LMW pools of LRRK2 and their associated kinase activity from whole-cell lysates. (A) Transiently transfected myc-LRRK2 from whole-cell lysates is present in two distinct pools, as assessed by glycerol velocity gradients: LMW and HMW. Glycerol gradients were calibrated using commercially available proteins with known molecular weights. Western blots from glycerol gradient fractions show that LMW LRRK2 migrates at ~230000, likely representing a monomer, while HMW LRRK2 is found at approximately double the molecular weight (~440000), consistent with a dimer. Addition of 0.5% SDS prior to glycerol gradients collapses HMW LRRK2. (B) Endogenous LRRK2 from human lymphoblasts is present in two distinct pools (LMW and HMW), similar to transfected LRRK2. Western blots from glycerol gradient fractions were probed with anti-myc (A) and anti-LRRK2 antibodies (B). (C) Endogenous γ-secretase complex, a protease of 230000−250000, is present in the same glycerol gradient fractions (15−19%) as LMW LRRK2. Cell lysates of HEK293FT cells transfected with myc-LRRK2 were separated using glycerol velocity gradients and analyzed using Western blots for endogenous components of the γ-secretase complex. Immature nicastrin (iNCT) undergoes further glycosylation to generate mature nicastrin (mNCT); only mNCT is part of the fully assembled γ-secretase complex. The N-terminal fragment of presenilin (NTF) is also selectively present in the fully assembled γ-secretase complex. Mitochondrial complex I (980000) is found in 35% glycerol, as evidenced by the presence of one its subunits, endogenous NDUFA9. (D) Chemical cross-linking of live cells leads to the formation of HMW complexes of endogenous LRRK2. Live lymphoblasts expressing endogenous LRRK2 were cross-linked with increasing concentrations of DSS, leading to a dose-dependent formation of SDS-stable HMW LRRK2 complexes. (E) HMW LRRK2 is more active than LMW LRRK2. Wild-type myc-LRRK2 from transfected HEK293FT cells was separated into LMW and HMW pools using glycerol gradients, IPed using myc resin, and subjected to an autophosphorylation assay of kinase activity. An autoradiograph of an SDS−PAGE gel separating the LRRK2 kinase reaction products shows increased levels of incorporation of radioactive ^{32}P into HMW LRRK2 compared to LMW LRRK2. Similar levels of LRRK2 were present in both reaction mixtures, as analyzed by Western blot. The relative kinase activity of HMW LRRK2 is 8.4-fold greater than that of LMW LRRK2 (mean ± standard error of the mean, $p = 0.03$, $n = 6$, unpaired t test). The asterisk indicates $p < 0.05$.

Statistical Analyses. Data were analyzed either by a two-tailed Student's t test (Figures 2 and 3) or by an unpaired two-tailed t test with unequal variance (Figures 1, 4, and 7). The latter was used when data were normalized to control (*36*).

Mice. All animals were housed and cared for under the guidelines established by Harvard University's Institutional Animal Care and Use Committees in compliance with federal standards and fed standard chow. Cytosolic and membrane fractions were prepared from brains of C57BL/6 mice that were 16 months of age, as described above.

RESULTS

Two Pools of LRRK2 with Distinct Molecular Weights Are Observed from Whole-Cell Extracts. To biochemically separate independent forms of LRRK2, we employed glycerol velocity gradients (*37*), which separate native proteins on the basis of relative buoyancy (molecular weight and hydrodynamic

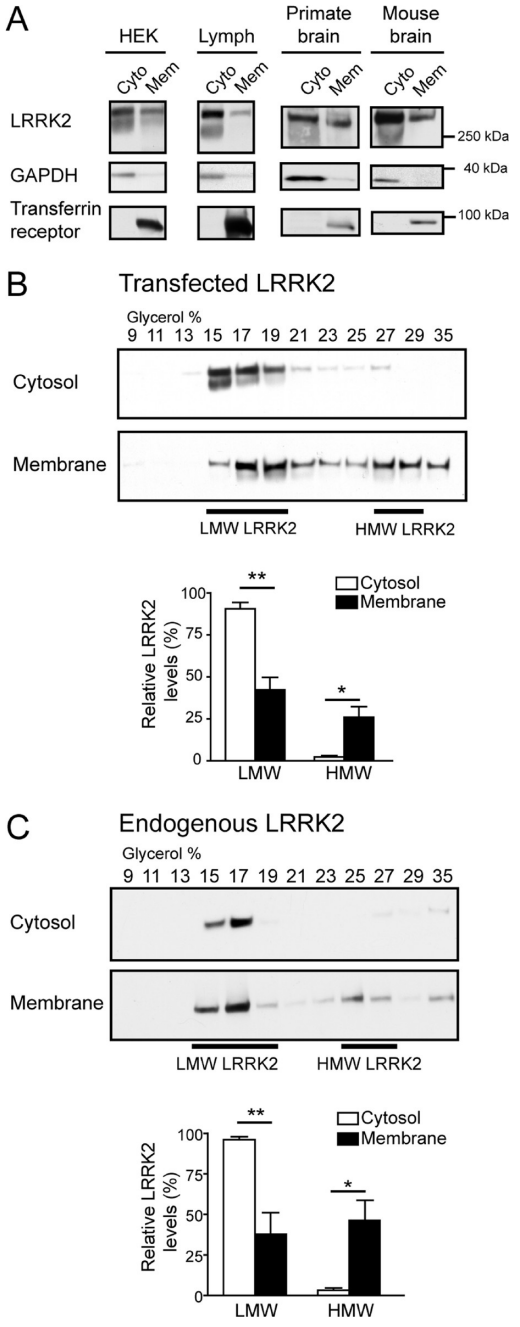

FIGURE 2: High-molecular weight LRRK2 complex is enriched at the membrane. (A) A higher proportion of LRRK2 is localized in cytosol than at the membrane. HEK293FT cells (HEK), lymphoblasts (Lymph), and primate or mouse brains were homogenized and fractionated into cytosol (Cyto) and membrane (Mem) fractions. Both fractions were volume-normalized and analyzed by SDS–PAGE and Western blot. GAPDH and the transferrin receptor were used as controls for proteins in the cytosol and membrane fractions, respectively. (B) Glycerol gradients of cytosol and membrane extracts from HEK293FT cells transfected with myc-LRRK2 reveal a 20-fold enrichment of HMW LRRK2 at the membrane compared to the cytosol ($p = 0.02$). A higher proportion of LMW LRRK2 is found in the cytosol than in the membrane compartment (mean ± standard error of the mean, $p = 0.004$, $n = 4$, Student's t test). One asterisk indicates $p < 0.05$, and two asterisks indicate $p \leq 0.01$. (C) Analysis of endogenous LRRK2 from human lymphoblasts reveals an enrichment of its HMW complex at the membrane, similar to that observed in panel B with transfected LRRK2. The levels of HMW LRRK2 are 15-fold higher in membrane than cytosolic fractions (mean ± standard error of the mean, $p = 0.01$, $n = 4$, Student's t test). One asterisk indicates $p < 0.05$, and two asterisks indicate $p \leq 0.01$.

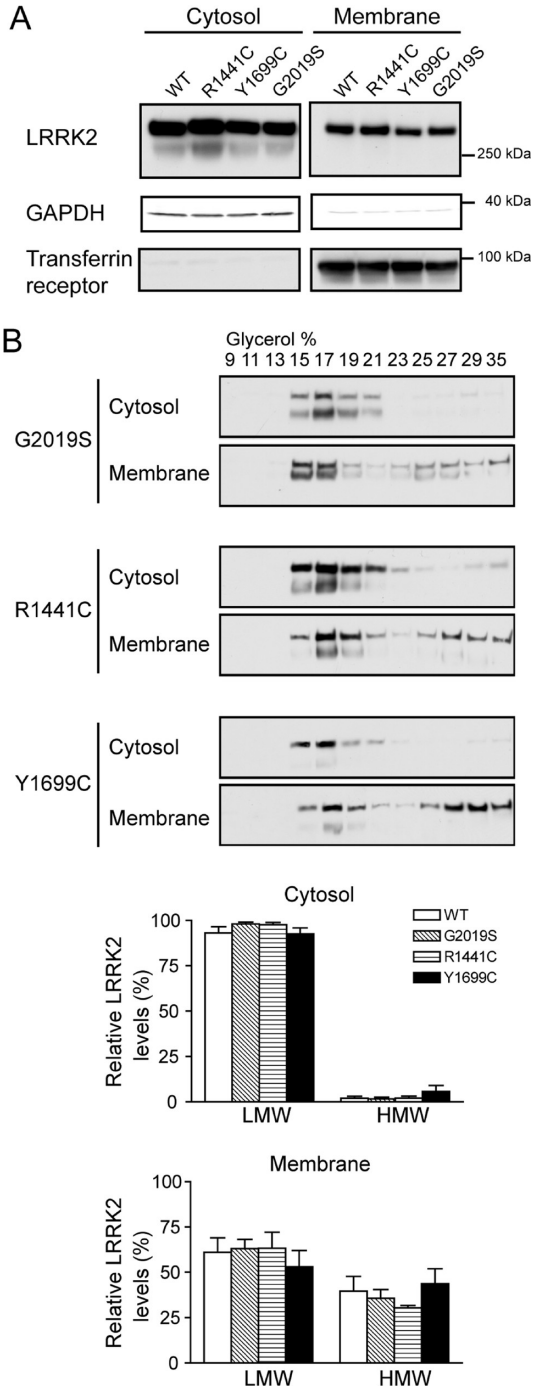

FIGURE 3: PD-linked mutants do not influence the subcellular localization or oligomerization state of LRRK2. (A) PD-linked LRRK2 mutants and wild-type LRRK2 show similar distributions across the cytosol and membrane compartments when expressed in HEK293FT cells. (B) Glycerol gradients of cytosol and membrane fractions from HEK293FT cells transfected with PD-linked LRRK2 mutants. The distribution of LMW and HMW LRRK2 in either cytosol or membrane fractions is not significantly changed by the introduction of PD-linked LRRK2 mutations (G2019S, R1441C, and Y1699C) (mean ± standard error of the mean, $n = 3$, Student's t test, all $p > 0.05$).

radius). Analysis of total extracts from HEK293FT cells transfected with human wild-type full-length LRRK2 (myc-tagged) revealed a biphasic distribution of LRRK2 across the gradient (Figure 1A). We termed these two distinct pools low-molecular weight (LMW) and high-molecular weight (HMW) LRRK2. LMW LRRK2 migrates at ~230000, likely representing a monomer,

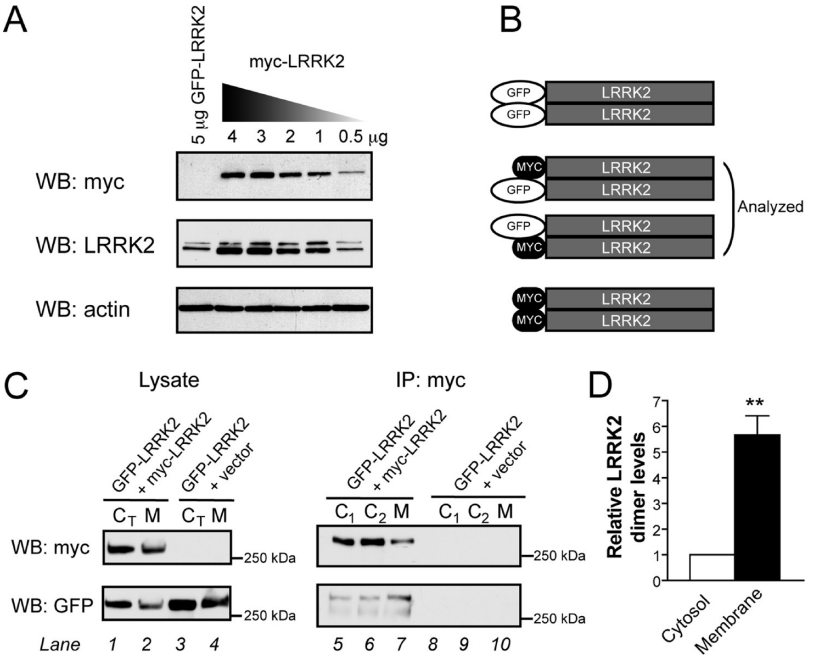

FIGURE 4: Heterologous co-immunoprecipitation confirms an enrichment of the LRRK2 dimer at the membrane. (A) To optimize the heterologous co-immunoprecipitation (co-IP) system, the amount of myc-LRRK2 DNA was titrated to match the expression levels of GFP-LRRK2. Transfection with 0.5 μg of myc-LRRK2 led to similar levels of LRRK2 protein as 5 μg of GFP-LRRK2. (B) Schematic depicting possible LRRK2 dimers after transfection with GFP-LRRK2 and myc-LRRK2 plasmids. Co-IP of heterologously tagged constructs allows quantification of the GFP-LRRK2−myc-LRRK2 heterodimer, which at equal levels of both proteins will likely represent 50% of the total dimer. (C) Cytosol and membrane fractions from cells co-expressing GFP-LRRK2 and myc-LRRK2 (lanes 1 and 2) or GFP-LRRK2 and an empty vector (lanes 3 and 4) were used for IP using a high-affinity myc resin. GFP-LRRK2 is co-IPed only in the presence of myc-LRRK2 (lanes 5−10), confirming the specificity of IP. Higher levels of GFP-LRRK2 are pulled down from membrane extracts (lane 7), despite lower levels of myc-LRRK2 in the same IP, suggesting an enrichment of the LRRK2 dimer at the membrane. Identical results from two independent samples (C_1 and C_2) using the same total cytosolic fraction (C_T) illustrate the low variability of this assay. (D) Levels of LRRK2 heterodimers are 5.7-fold higher in membrane extracts (mean ± standard error of the mean, $p = 0.01$, $n = 3$, unpaired t test). The relative dimer levels were quantified by measurement of the band intensity of co-IPed GFP-LRRK2 divided by the intensity of IPed myc-LRRK2. The value for cytosol was arbitrarily set to 1. Asterisks indicate $p \leq 0.01$.

while HMW LRRK2 is found at approximately double the molecular weight (~440000), consistent with a LRRK2 dimer (Figure 1A). The apparent migration of the LRRK2 monomer and dimer slightly below their predicted molecular weights is likely due to the dependence of sedimentation velocity on the hydrodynamic radius of the protein.

Endogenous LRRK2 from human lymphoblasts displayed a nearly identical distribution, with two distinct pools of LRRK2 (Figure 1B). Since LRRK2 in the lymphoblasts is expressed at several-fold lower levels than that following transient transfection (Figure S1A of the Supporting Information), these data suggest that the distribution of LRRK2 across the glycerol gradient is not influenced by protein expression levels. The occasional shift in LMW or HMW LRRK2 by one fraction is likely due to the subtle variability of manual fraction collection. A similar LRRK2 distribution was observed in whole-cell lysates from the dopaminergic MES cell line transfected with LRRK2 (Figure S1B of the Supporting Information) as well as when using multiple nonionic detergents [0.1−0.5% Triton X-100 and 0.5% DDM (data not shown)]. The addition of the denaturing detergent, SDS, to cell lysates prior to separation resulted in a complete collapse of HMW LRRK2 (Figure 1A,B, bottom panels), consistent with HMW LRRK2 representing a dissociable, multimeric protein complex. The relative abundance of the LMW and HMW pools of LRRK2 observed by glycerol gradient separation is also consistent with the low levels of oligomeric LRRK2 determined using heterologous co-immunoprecipitation from whole-cell lysates (Figure S1C of the Supporting Information).

To confirm the calibration of the glycerol gradients that was accomplished using commercial protein standards, we analyzed the sedimentation of two well-characterized, endogenous protein complexes in the same glycerol gradients. The endogenous γ-secretase complex is a 230000−250000 protease as determined by Blue-Native PAGE, glycerol gradients, and scanning eletron transmission microscopy (*38*−*40*) and is readily identified by the presence of both a mature glycosylated form of nicastrin (mNCT) and presenilin N-terminal fragment (NTF) (*41*, *42*). Fully assembled γ-secretase was found in the 15−19% glycerol fractions (Figure 1C), similar to LMW LRRK2 (Figure 1A,B) and consistent with the calibration with multiple protein standards. Endogenous mitochondrial complex I, a 980000 multiprotein complex (*43*), was detected in 35% glycerol (Figure 1C), consistent with our prior calibration with the protein standards. To further confirm that LMW and HMW LRRK2 represented LRRK2 monomer and dimer, respectively, HEK293FT cells were transiently cotransfected with myc-LRRK2 and GFP-LRRK2 and cell lysates were separated with a glycerol gradient. LMW and HMW fractions were then IPed using a high-affinity myc resin and probed using myc and GFP antibodies. Substantially more GFP-LRRK2 was co-IPed from the HMW than from the LMW fractions (Figure S1D of the Supporting Information), confirming that HMW LRRK2 represents the LRRK2 dimer. Consistent with this observation, LRRK2 collected from the HMW glycerol gradient fractions is efficiently cross-linked into

covalent HMW SDS-stable complexes while LMW LRRK2 is not (Figure S2A of the Supporting Information).

Endogenous and transfected LRRK2 has been repeatedly observed by us (e.g., Figure 1) and others (*12*, *28*, *29*) as two distinct bands on a Western blot. Since both bands could be detected with antibodies against both extreme C-terminal (proprietary anti-LRRK2 antibody) and two different N-terminal antibodies (monoclonal and polyclonal anti-myc), they must both represent the full-length LRRK2 protein (data not shown). Dephosphorylation did not affect the band migration, and both bands could be observed when blotting extracts from in vitro transcription/translation of LRRK2 using rabbit reticulocytes (data not shown), indicating that post-translational modifications are unlikely to cause this effect. In all experiments, both bands representing the full-length LRRK2 protein were considered and quantified, if present.

To confirm the presence of multiple oligomerization states of LRRK2 by an independent method, we used live-cell cross-linking, which covalently stabilizes proteins in the proximity into SDS-stable complexes which can be readily resolved by SDS−PAGE or Western blotting. The cross-linking of live human lymphoblasts (using DSS) expressing endogenous LRRK2 led to the formation of HMW LRRK2 complexes even at relatively low (25 μM) concentrations of DSS (Figure 1D), consistent with an efficient cross-linking reaction. The same cross-linker had similar effects in live MES cells transfected with LRRK2 (Figure S2B of the Supporting Information). SDS-stable complexes migrating at similar molecular weights were also obtained following live-cell cross-linking with several other reagents (BMOE, BMH, DST, and SATP), which possess different functional groups (amine and sulfhydryl) and various spacer arm lengths [4.1−16.1 Å (Figure S2C of the Supporting Information)]. These data show that both endogenous and exogenous LRRK2 form multiple HMW complexes in live cells, indicative of multiple protein−protein interactions. These likely include interactions with other LRRK2 molecules, as well as other proteins. The presence of multiple complexes observed following cross-linking compared to the biphasic distribution of LRRK2 from the glycerol velocity gradients may reflect the ability of cross-linkers to capture both more transient and weaker interactions of LRRK2 (e.g., with substrates, cofactors, and chaperones) but confirm the putative dimer as the major HMW species.

To examine the functional consequences of these results, we utilized a well-described LRRK2 autophosphorylation assay (*12*, *13*, *15*, *28*). Using whole-cell lysates from transfected cells, we observed an approximately 2-fold increase in kinase activity of the G2019S mutation compared to WT LRRK2 and a lack of kinase activity of the kinase-dead construct (Figure S2D of the Supporting Information), consistent with previous reports (*12*, *13*, *15*, *28*) and validating the assay in our hands. To analyze the functional consequences of LRRK2 dimer assembly, the same assay was used to compare the specific activity of LMW and HMW LRRK2 extracted from whole-cell extracts, following their separation via glycerol velocity gradients. We observed an 8.4-fold increase in relative LRRK2 activity in the HMW fraction (Figure 1E), consistent with a recent publication reporting the increased activity of the G2019S mutant LRRK2 dimer compared to that of the mutant monomer (*44*).

High-Molecular Weight LRRK2 Is Enriched at the Membrane. Previous reports have demonstrated the presence of LRRK2 in both cytosol and membrane fractions (*21*, *22*), although the relative distribution has not been well characterized. Therefore, we fractionated cells and tissue into cytosol and membrane pools, volume-adjusted both fractions, and determined the relative abundance of soluble or membrane-associated LRRK2. Analysis of HEK293FT cells transfected with LRRK2 showed that the majority of cellular LRRK2 was present in the cytosol (~75%) with a smaller amount (~25%) at the membrane. A similar distribution was observed with endogenous LRRK2 from human lymphoblasts and primate and mouse brain (Figure 2A). These data indicate that in our experimental systems, the majority of LRRK2 is present in cytosol with a smaller proportion localized to the membrane.

Next, we examined if LMW or HMW LRRK2 is preferentially enriched in either subcellular fraction. Analysis of HEK293FT cells transfected with LRRK2 revealed the presence of LMW LRRK2 in both fractions while HMW LRRK2 was almost exclusively present at the membrane (Figure 2B). Quantification of multiple experiments showed a 20-fold enrichment of HMW LRRK2 at the membrane (Figure 2B). Similar results were observed with endogenous LRRK2, with a 15-fold enrichment (Figure 2C). To determine if PD-linked mutations exhibited differences from the wild-type protein, we analyzed both the relative distribution in cytosolic and membrane fractions (Figure 3A and Figure S3A of the Supporting Information) and LMW versus HMW distribution across the glycerol gradients (Figure 3B). Interestingly, no significant differences were observed either in cytosol or in membrane fractions via analysis of the R1441C, Y1699C, and G2019S PD-linked mutations, which occur in three distinct domains of LRRK2 (Figure 3).

To verify the enrichment of HMW LRRK2 at the membrane using an independent method, we employed co-immunoprecipitation (co-IP) of heterologously tagged LRRK2 constructs. Expression levels of myc-LRRK2 and GFP-LRRK2 were matched in prior experiments (Figure 4A), maximizing the probability of forming GFP-LRRK2−myc-LRRK2 heterodimers (Figure 4B). Both GFP-LRRK2 and myc-LRRK2 were present at higher levels in the cytosol than at the membrane (Figure 4C, lanes 1 and 3), illustrating that LRRK2 localization is tag-independent and again that the majority of total LRRK2 is found in the cytosol. The previously observed ratio of soluble to membrane-associated LRRK2 was preserved in the myc immunoprecipitations (IPs) (Figure 4C, lanes 5−7), suggesting that the high-affinity anti-myc resin exhibited a similar capture efficiency in both fractions.

If equal amounts of the LRRK2 dimer were present in cytosol and membrane fractions, one would expect the levels of co-IPed GFP-LRRK2 to mirror the pattern of myc-LRRK2: higher levels of GFP-LRRK2 from the cytosol and lower levels from membranes. However, the opposite was observed. The myc resin pulled down more GFP-LRRK2 from the membrane than from the cytosol (Figure 4C, lane 7 vs lanes 5 and 6), consistent with a greater abundance of the LRRK2 dimer in the membrane fraction. This was observed despite lower levels of IPed myc-LRRK2 in this fraction (Figure 4C, lane 7). Since the relative amounts of the dimer can be quantified by using the GFP-LRRK2:myc-LRRK2 ratio in the IP, an analysis across three independent experiments revealed a 5.7-fold enrichment of LRRK2 dimer in the membrane fraction compared to the cytosol (Figure 4D).

To further confirm that the HMW LRRK2 complexes were enriched at the membrane, we compared the relative efficiency of LRRK2 cross-linking in cytosol and membrane fractions using increasing concentrations of DSS. No cross-linking of endogenous LRRK2 was observed in the cytosolic fraction from lymphoblasts

up to 50 μM DSS, while LRRK2 from the membrane fraction was efficiently cross-linked into HMW complexes (Figure 5A).

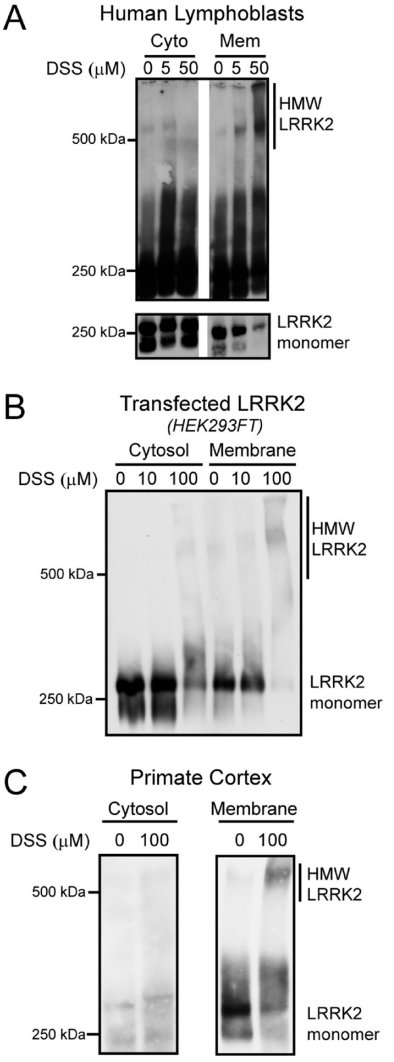

FIGURE 5: Membrane-bound LRRK2 can be cross-linked more efficiently into HMW complexes than cytosolic LRRK2. Cross-linking with DSS of endogenous or transfected LRRK2 leads to formation of HMW complexes in membrane fractions (Mem), but not in cytosol (Cyto). Extracts from human lymphoblasts (A), HEK293FT cells transfected with LRRK2 (B), and non-human primate cortex (C) were analyzed.

Efficient cross-linking of LRRK2 into HMW complexes was also observed in membrane extracts from HEK293FT cells transfected with LRRK2 (Figure 5B), and from non-human primate brain extracts (Figure 5C). In contrast, LRRK2 from the cytosolic fractions consistently failed to cross-link at these concentrations (Figure 5B,C). Thus, glycerol velocity gradients, heterologous co-IP, and cross-linking all support the enrichment of the HMW LRRK2 kinase complex at the membrane with both endogenous and exogenous LRRK2 from cells and brain tissue.

There are conflicting reports about the estimated size of LRRK2 using size exclusion chromatography (SEC). While some groups have found LRRK2 to elute at ~600000 (*28*, *45*), the data of others suggest that most of LRRK2 elutes at a much larger size (*44*, *46*). However, one report analyzed further this very large LRRK2 pool and concluded that it was a monomer and that monomeric LRRK2 elutes aberrantly via SEC (*46*). Our SEC analysis of LRRK2 from cytosol, which contains almost exclusively LRRK2 monomer, suggested a molecular weight of ~1300000 (Figure 6A), consistent with this prior report. Furthermore, a similar elution profile was observed when the LMW fraction from the glycerol gradient was subsequently analyzed by SEC (Figure 6A). In our hands, HMW LRRK2 eluted at ~500000, consistent with the approximate molecular weight of the LRRK2 dimer and the prior observations that LRRK2 dimer may elute properly on SEC (*46*), despite the unexpected behavior of the monomer. Since we report that most of LRRK2 is present as a monomer in transfected cells, most LRRK2 from whole-cell lysates would be expected to elute as the "abnormal" large complex, consistent with a prior report (*44*). We have also confirmed the apparent size of LMW and HMW LRRK2 as monomer and dimer, respectively, using Blue-Native PAGE calibrated with two different commercial molecular weight standards (Figure 6B and Figure S4A of the Supporting Information). This indicates that SEC may uniquely report an inaccurate weight of monomeric LRRK2. To address the apparent discrepancies of LRRK2 size between multiple groups (~1300000 vs 600000) using size exclusion chromatography, we compared the elution profiles of LRRK2 from cytosol using our conditions with those previously used to estimate the LRRK2 molecular weight of ~600000 (*28*, *45*). Comparison of the LRRK2 elution profile in the absence or presence of Triton-X100 revealed that the addition of the detergent leads to a broader elution peak for LRRK2, thus changing its estimated molecular weight (Figure S4B of the Supporting Information), potentially accounting for

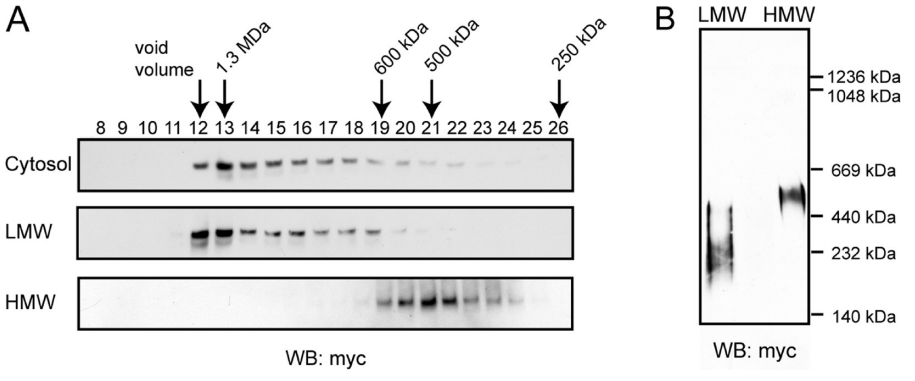

FIGURE 6: Analysis of LRRK2 by size exclusion chromatography and Blue-Native PAGE. (A) Cytosolic LRRK2 and LMW LRRK2 (both monomers) elute similarly from a Superdex 200 column, at ~1300000, while HMW LRRK2 (LRRK2 dimer) elutes at ~500000. (B) LMW LRRK2 from the glycerol gradient separation subsequently migrates on BN-PAGE as a LRRK2 monomer, whereas migration of HMW LRRK2 corresponds to a dimer. Two commercially available molecular weight standards were used on the Blue-Native PAGE to estimate the LRRK2 molecular weight (see Figure S4 of the Supporting Information).

some of the differences reported by various groups analyzing LRRK2 via SEC.

LRRK2 Localization Affects Its Activity and Biochemical Properties. To examine the functional consequences of LRRK2 localization, we utilized the well-documented LRRK2 autophosphorylation assay. We prepared cytosol and membrane fractions, IPed equal amounts of LRRK2 from both, and compared their relative in vitro LRRK2 kinase activities. Analysis of three independent experiments revealed a 3.1-fold increase in the relative autophosphorylation activity of membrane-associated LRRK2 compared to cytosolic LRRK2 (Figure 7A). Kinase-dead LRRK2, which was present in both cytosol and membrane fractions (Figure S3B of the Supporting Information), did not exhibit significant activity from either fraction (Figure S5A of the Supporting Information), confirming the specificity of the assay. Similar increases in membrane-associated kinase activity were also observed in a second assay, using myelin basic protein as a pseudosubstrate (Figure S5B of the Supporting Information). However, this assay was not exhaustively employed because of the greater variability and considerably weaker specificity for LRRK2 activity that we (not shown), and others (*28*), have observed.

LRRK2 can bind GTP through its COR domain (*13*, *17*, *34*, *47*, *48*), and GTP binding may influence the kinase activity of LRRK2 (*13*, *49*). To further biochemically characterize cytosolic and membrane pools of LRRK2, we compared the relative binding of LRRK2 to GTP-agarose beads using a previously established assay (*13*, *17*, *34*, *47*, *48*). Endogenous membrane-associated LRRK2 from lymphoblasts and primate brain exhibited stronger binding to GTP resin than cytosolic LRRK2 (Figure 7B,C and Figure S5C,D of the Supporting Information). Similar results were also obtained with extracts from dopaminergic MES cells transfected with WT-LRRK2 (Figure S5E of the Supporting Information).

Kinases are often regulated by phosphorylation (*50*−*52*), and indeed, multiple phosphorylation sites have been identified in LRRK2 (*53*, *54*). In the absence of phospho-specific LRRK2 antibodies, we evaluated the overall extent of LRRK2 phosphorylation in cytosolic and membrane fractions using an organic fluorophore, Pro-Q Diamond, which binds to the phosphate moiety in a manner independent of the protein context (*55*). LRRK2 was IPed from both cytosolic and membrane fractions and separated via SDS−PAGE, and the LRRK2 protein was first stained with Pro-Q Diamond Phosphoprotein stain and subsequently analyzed with a total protein stain (Figure 7D). The levels of phospho-LRRK2 were normalized to total LRRK2 to obtain the relative phosphorylation levels. Quantitative analysis of three independent experiments showed that membrane-associated LRRK2 was phosphorylated to a lesser extent (−31%) than cytosolic LRRK2 (Figure 7D).

DISCUSSION

Previous studies have established that LRRK2 is a bona fide kinase (*12*, *13*, *15*, *28*), and more recent evidence suggests that it exists as a dimer (*28*−*30*). Here we report that the less abundant LRRK2 dimer is more active than the more abundant monomer. Since LRRK2 is thought to localize to membranous structures in mammalian brain (*21*), we hypothesized that control over subcellular localization may represent a mechanism for regulating LRRK2 function. Here, we report that the membrane association of LRRK2 is accompanied by a number of different but likely related biochemical events. These include an increased level of dimerization, an increased kinase activity, an increased level of GTP binding, and a decreased level of phosphorylation (compared to those of cytosolic LRRK2). In summary, our data suggest that membrane targeting and dimerization of wild-type LRRK2 are critical biochemical mechanisms governing LRRK2 kinase activity, and therefore its function within the cell.

The difference in activity between cytosolic and membrane-associated wild-type LRRK2 (~3-fold) is comparable to that between the wild type and the pathogenic G2019S mutant in whole-cell lysates. This suggests that the association of LRRK2 with membranes may be as influential with respect to LRRK2 function as at least one pathogenic mutation and could represent a key event in the regulation of LRRK2 activity. Also, HMW LRRK2 is ~8-fold more active than LMW, suggesting that the HMW pool represents an "activated" state and that the increased kinase activity of membrane-associated LRRK2 is likely at least partly due to an enrichment of the highly active dimer.

The increased activity of membrane-associated LRRK2 was also accompanied by strengthened GTP binding of endogenous LRRK2 extracted from human lymphoblasts and primate cortex. This observation may be a result of an increased level of GTP exchange, a tendency toward increased GTPase activity, or a relatively GTP-deficient state of the membrane-associated LRRK2 protein. However, these were not directly addressed in this work. Future experiments will examine these possible mechanisms, as well as the relative GTPase activities of cytosolic and membrane-associated LRRK2, and kinetics parameters of these biochemically distinct pools of LRRK2, as recently reported (*56*−*58*).

We report decreased phosphorylation activity of the membrane-associated LRRK2 compared to cytosolic LRRK2, which suggests that dephosphorylation at certain sites may represent a requisite step in increased LRRK2 activity, dimer formation, trafficking to the membrane, or a combination of these processes. These data are consistent with a widely accepted model in which phosphorylation of kinases regulates their function (*50*−*52*). Importantly, since LRRK2 is a large kinase with 103 predicted phosphorylation sites [77 Ser, 15 Thr, and 11 Tyr residues (http://www.cbs.dtu.dk/services/NetPhos/)] (*59*), the ~30% decrease in the level of membrane LRRK2 phosphorylation may represent a major change in a small subset of these sites, which may correlate with subcellular localization. Future analysis of specific LRRK2 phosphorylation sites (*53*, *54*) using mass spectrometry or LRRK2 phospho-specific antibodies may help identify which amino acid residues are involved in these processes and dissect the precise consequences of their phosphorylation on LRRK2 function.

Several studies have analyzed the molecular weight distribution of LRRK2 by size exclusion chromatography (SEC) with varying results. While some have reported substantial levels of LRRK2 above 1000000, all groups have failed to observe a pool of LRRK2 at the predicted molecular weight of a monomer. Early studies thus concluded that most LRRK2 exists as a HMW complex (*28*, *45*). However, recent work has analyzed the very HMW LRRK2 species and concluded that it is in fact an anomalously eluting monomer (*46*), consistent with our SEC data (Figure 6 and Figure S4 of the Supporting Information) and glycerol velocity gradient analyses (Figures 1 and 2). In addition, our data reporting an ~8-fold greater kinase activity of the LRRK2 dimer compared to that of the monomer (separated by glycerol gradients) are consistent with the work from another group that found an ~6-fold greater kinase activity of the

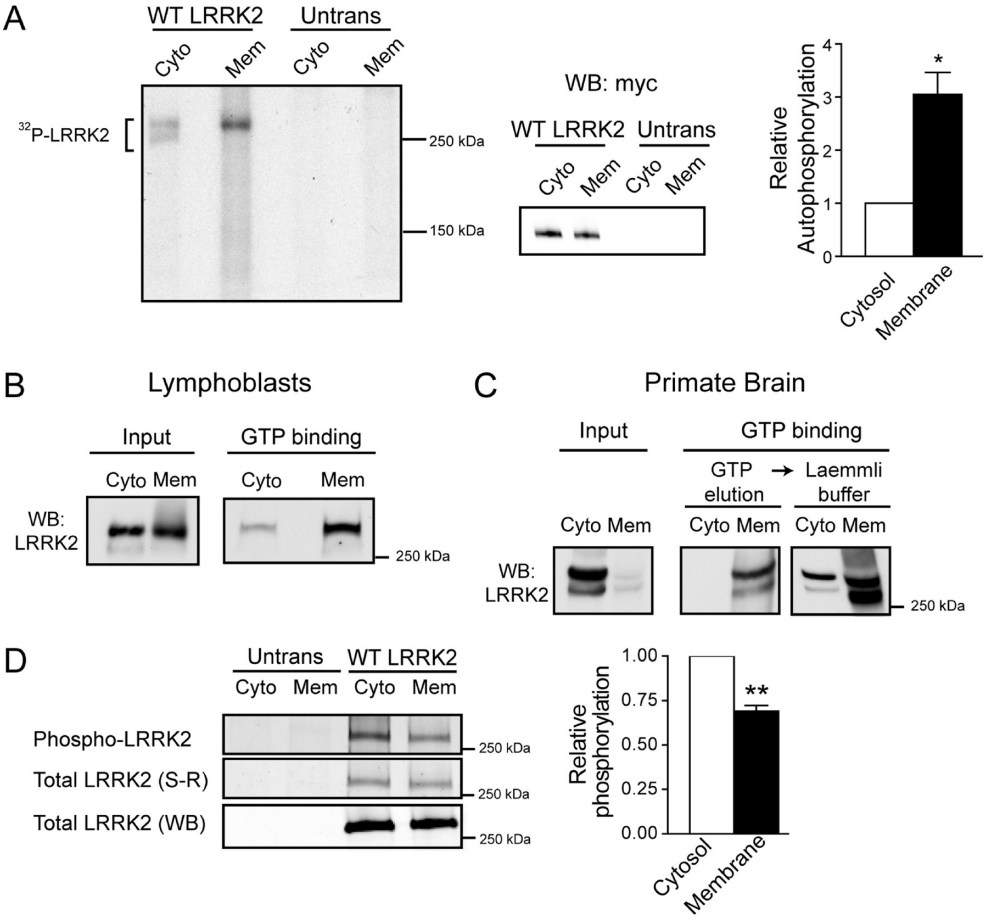

FIGURE 7: Membrane-associated LRRK2 is biochemically distinct from cytosolic LRRK2. (A) Membrane-associated LRRK2 exhibits greater in vitro kinase activity than cytosolic LRRK2. Cytosol and membrane fractions from HEK293FT cells transfected with wild-type myc-LRRK2 or from untransfected cells (Untrans) were used for myc IP and the subsequent LRRK2 autophosphorylation assay. Membrane and cytosolic fractions were normalized to achieve similar levels of LRRK2 in the kinase reaction mixture, shown by Western blot. An autoradiograph of an SDS−PAGE gel separating the LRRK2 autophosphorylation reaction products shows an increased level of incorporation of radioactive ^{32}P into LRRK2 from membrane extracts. LRRK2 from the cytosolic fraction migrates on this gel as a doublet; both bands correspond to full-length LRRK2 and were included in the analysis. Relative LRRK2 kinase activity is 3.1-fold greater from membrane fraction than from cytosol (mean ± standard error of the mean, $p = 0.04$, $n = 3$, unpaired t test). The asterisk indicates $p < 0.05$. (B) Membrane-associated LRRK2 from human lymphoblasts binds GTP more efficiently than cytosolic LRRK2. The levels of LRRK2 were normalized in the input, and equal volumes of inputs were used for each analysis, with three independent experiments demonstrating similar results. (C) Membrane-associated LRRK2 extracted from primate brain binds GTP more efficiently than cytosolic LRRK2. LRRK2 was first eluted with GTP from the resin, and subsequently, the GTP binding resin was boiled in Laemmli buffer. Samples used for the assay were protein and volume normalized, and a representative experiment ($n = 3$) is shown. (D) Membrane-associated LRRK2 is phosphorylated to a lesser extent than cytosolic LRRK2. Cytosolic and membrane fractions from untransfected cells (Untrans) or cells transfected with wild-type myc-LRRK2 (WT LRRK2) were IPed with myc resin and analyzed for phosphorylation using Pro-Q Diamond Phosphoprotein gel stain (Phospho-LRRK2). The relative levels of LRRK2 phosphorylation were quantified by normalization of the intensity of phospho-LRRK2 (phosphoprotein stain) to the levels of total LRRK2 protein by SYPRO Ruby stain (total LRRK2 S-R). Relative LRRK2 levels were further confirmed via analysis of a small aliquot of each fraction by Western blot (total LRRK2 WB) (mean ± standard error of the mean, $p = 0.01$, $n = 3$, unpaired t test). Asterisks indicate $p \leq 0.01$.

LRRK2 dimer compared to very HMW LRRK2 from the SEC void volume, which we (Figure 6 and Figure S4 of the Supporting Information) and others have likewise defined as monomer (*46*). On the basis of the data obtained from multiple separation methods, we speculate that the LRRK2 monomer may exist as a relatively diffuse structure whereas the LRRK2 dimer may possess a more compacted/globular structure more amenable to separation via SEC. This interpretation is analogous to the aberrant migration of linear dextran standards compared to biological protein standards. While the LRRK2 monomer was identified by glycerol velocity gradients and Blue-Native PAGE, and subsequently confirmed by heterologous co-IP and cross-linking, the aberrant migration of the LRRK2 monomer observed by us and others will warrant further examination.

Interestingly, the G2019S mutant shows increased kinase activity (Figure S2D of the Supporting Information and refs *12*, *13*, *15*, and *28*) without detectable changes in its subcellular localization or LMW versus HMW distribution (Figure 3). This is likely due to the fact that the G2019 residue sits within the kinase domain and directly affects the kinetic properties of the kinase moiety. While a previous study using full-length and truncated LRRK2 species suggested that the R1441C mutation may destabilize a LRRK2 heterodimer (*31*), we did not observe any significant differences in HMW/dimer levels using three various full-length PD-linked mutants (including R1441C), suggesting that mutations in the context of full-length LRRK2 may not lead to substantially different dimer levels at the steady state. Our data contrast with a previous report (*44*) suggesting differences between the wild type and G2019S in the levels of their respective dimers. These differences may be attributed to differences in the extraction protocol; we used detergents to extract membrane-associated LRRK2 (the major source of LRRK2

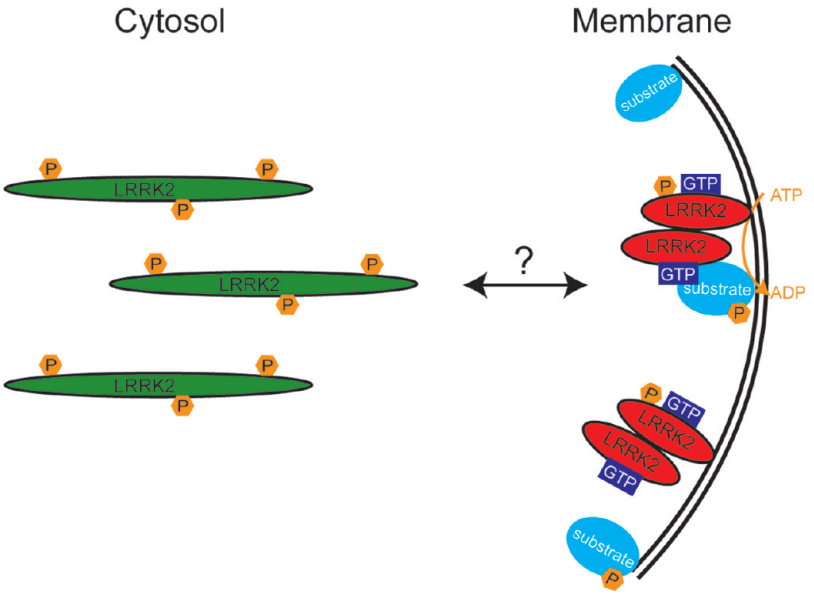

FIGURE 8: Schematic representation of the proposed model of LRRK2 dimer assembly and kinase regulation. Using both endogenous and exogenous LRRK2, we have observed that membrane-associated LRRK2 is substantially enriched for LRRK2 dimer, whereas cytosolic LRRK2 is present mostly as a monomer. Membrane-associated LRRK2 possesses greater kinase activity and a stronger propensity to bind GTP and is relatively dephosphorylated, compared to cytosolic LRRK2. We propose a model in which LRRK2 exists mostly as a monomer in the cytosol that can translocate to the membrane where it dimerizes, becomes more active, and subsequently phosphorylates its substrates. The similarities of this model to the established regulation of other kinases (and GTPases) suggest that membrane translocation and dimerization may be reversible and tightly controlled.

dimer), while the previous report employed cycles of freezing and thawing in a detergent-free condition, which may not completely extract LRRK2 from the membrane, thus accounting for the observed differences. However, we cannot rule out the possibility that smaller differences between wild-type LRRK2 and mutants exist or that other related features, such as the kinetics of dimerization or the intrinsic stability of PD-linked mutant dimers, may differ.

Our observation of greater in vitro LRRK2 kinase activity in membrane preparations leads us to speculate that the membrane compartment is likely the site where LRRK2 exerts its physiologically relevant function in the cell. Indeed, many cellular processes that are influenced by LRRK2 occur at the membrane or involve membrane dynamics (*23*−*27*, *60*). We suggest that LRRK2 is predominantly found as a monomer in the cytosol but can translocate to the membrane, subsequently dimerize, and thus possesses greater kinase activity (Figure 8). This LRRK2 model is similar to that of a well-studied canonical MAPKKK Raf, which can phosphorylate its target proteins at the membrane and is regulated by dimerization, membrane association, and phosphorylation (*52*, *61*).

Interestingly, the relatively small proportion of LRRK2 dimer in whole-cell extracts implies a low level of basal kinase activity. This interpretation is supported by the relatively low rate of ^{32}P incorporation in various LRRK2 kinase assays and consistent with the relatively low basal (unstimulated) activity of other MAPKKKs (*52*). Therefore, identification of events leading to membrane translocation and/or formation of the LRRK2 dimer may provide critical insights into LRRK2 biology. The discovery of such events may help uncover differences between wild-type and pathogenic LRRK2 proteins, which we (Figure 3) and others (*18*, *19*, *22*) have failed to observe at resting states with non-G2019S mutants. It is reasonable to suggest that membrane translocation and dimerization are reversible and regulated events, which represent key mechanisms for the cell to regulate LRRK2 activity. Since penetrance of the autosomally dominant inherited LRRK2 mutations is incomplete and age-dependent (*7*−*10*), regulation of LRRK2 activity is likely to be highly complex and potentially relevant to the emergence of PD pathogenesis.

In summary, we propose a novel mechanism of regulating LRRK2 function through its membrane localization and dimerization. Our findings have implications for the identification of substrates, the biochemical composition and nature of active LRRK2, and LRRK2 function within the cell. Additional work will be required, however, to elucidate the pathological relevance of these findings in the context of PD-linked mutants specifically within the neuronal environment.

ACKNOWLEDGMENT

We thank Dr. Mark Cookson (National Institute on Aging, Bethesda, MD) for providing the LRRK2 plasmids, the New England Primate Research Facility for providing the non-human primate cortex tissue, Drs. Justus Dächsel and Matthew J. Farrer for technical advice, and the Coriell Institute for Biomedical Research for providing lymphoblasts.

SUPPORTING INFORMATION AVAILABLE

Additional analyses of LRRK2 molecular weights, kinase activity, and GTP binding. This material is available free of charge via the Internet at http://pubs.acs.org.

REFERENCES

1. Thomas, B., and Beal, M. F. (2007) Parkinson's disease. *Hum. Mol. Genet. 16* (Special Issue No. 2), R183–R194.
2. Farrer, M. J. (2006) Genetics of Parkinson disease: Paradigm shifts and future prospects. *Nat. Rev. Genet. 7*, 306–318.
3. Cookson, M. R., Xiromerisiou, G., and Singleton, A. (2005) How genetics research in Parkinson's disease is enhancing understanding of the common idiopathic forms of the disease. *Curr. Opin. Neurol. 18*, 706–711.

4. Melrose, H. (2008) Update on the functional biology of Lrrk2. *Future Neurol. 3*, 669–681.
5. Paisan-Ruiz, C., Jain, S., Evans, E. W., Gilks, W. P., Simon, J., van der Brug, M., Lopez de Munain, A., Aparicio, S., Gil, A. M., Khan, N., Johnson, J., Martinez, J. R., Nicholl, D., Carrera, I. M., Pena, A. S., de Silva, R., Lees, A., Marti-Masso, J. F., Perez-Tur, J., Wood, N. W., and Singleton, A. B. (2004) Cloning of the gene containing mutations that cause PARK8-linked Parkinson's disease. *Neuron 44*, 595–600.
6. Zimprich, A., Biskup, S., Leitner, P., Lichtner, P., Farrer, M., Lincoln, S., Kachergus, J., Hulihan, M., Uitti, R. J., Calne, D. B., Stoessl, A. J., Pfeiffer, R. F., Patenge, N., Carbajal, I. C., Vieregge, P., Asmus, F., Muller-Myhsok, B., Dickson, D. W., Meitinger, T., Strom, T. M., Wszolek, Z. K., and Gasser, T. (2004) Mutations in LRRK2 cause autosomal-dominant parkinsonism with pleomorphic pathology. *Neuron 44*, 601–607.
7. Healy, D. G., Falchi, M., O'Sullivan, S. S., Bonifati, V., Durr, A., Bressman, S., Brice, A., Aasly, J., Zabetian, C. P., Goldwurm, S., Ferreira, J. J., Tolosa, E., Kay, D. M., Klein, C., Williams, D. R., Marras, C., Lang, A. E., Wszolek, Z. K., Berciano, J., Schapira, A. H., Lynch, T., Bhatia, K. P., Gasser, T., Lees, A. J., and Wood, N. W. (2008) Phenotype, genotype, and worldwide genetic penetrance of LRRK2-associated Parkinson's disease: A case-control study. *Lancet Neurol. 7*, 583–590.
8. Hulihan, M. M., Ishihara-Paul, L., Kachergus, J., Warren, L., Amouri, R., Elango, R., Prinjha, R. K., Upmanyu, R., Kefi, M., Zouari, M., Sassi, S. B., Yahmed, S. B., El Euch-Fayeche, G., Matthews, P. M., Middleton, L. T., Gibson, R. A., Hentati, F., and Farrer, M. J. (2008) LRRK2 Gly2019Ser penetrance in Arab-Berber patients from Tunisia: A case-control genetic study. *Lancet Neurol. 7*, 591–594.
9. Latourelle, J. C., Sun, M., Lew, M. F., Suchowersky, O., Klein, C., Golbe, L. I., Mark, M. H., Growdon, J. H., Wooten, G. F., Watts, R. L., Guttman, M., Racette, B. A., Perlmutter, J. S., Ahmed, A., Shill, H. A., Singer, C., Goldwurm, S., Pezzoli, G., Zini, M., Saint-Hilaire, M. H., Hendricks, A. E., Williamson, S., Nagle, M. W., Wilk, J. B., Massood, T., Huskey, K. W., Laramie, J. M., DeStefano, A. L., Baker, K. B., Itin, I., Litvan, I., Nicholson, G., Corbett, A., Nance, M., Drasby, E., Isaacson, S., Burn, D. J., Chinnery, P. F., Pramstaller, P. P., Al-hinti, J., Moller, A. T., Ostergaard, K., Sherman, S. J., Roxburgh, R., Snow, B., Slevin, J. T., Cambi, F., Gusella, J. F., and Myers, R. H. (2008) The Gly2019Ser mutation in LRRK2 is not fully penetrant in familial Parkinson's disease: The GenePD study. *BMC Med. 6*, 32.
10. Kay, D. M., Kramer, P., Higgins, D., Zabetian, C. P., and Payami, H. (2005) Escaping Parkinson's disease: A neurologically healthy octogenarian with the LRRK2 G2019S mutation. *Mov. Disord. 20*, 1077–1078.
11. Greggio, E., and Cookson, M. R. (2009) Leucine-rich repeat kinase 2 mutations and Parkinson's disease: Three questions. *ASN Neuro 1*, No. e00002.
12. West, A. B., Moore, D. J., Biskup, S., Bugayenko, A., Smith, W. W., Ross, C. A., Dawson, V. L., and Dawson, T. M. (2005) Parkinson's disease-associated mutations in leucine-rich repeat kinase 2 augment kinase activity. *Proc. Natl. Acad. Sci. U.S.A. 102*, 16842–16847.
13. Smith, W. W., Pei, Z., Jiang, H., Dawson, V. L., Dawson, T. M., and Ross, C. A. (2006) Kinase activity of mutant LRRK2 mediates neuronal toxicity. *Nat. Neurosci. 9*, 1231–1233.
14. Iaccarino, C., Crosio, C., Vitale, C., Sanna, G., Carri, M. T., and Barone, P. (2007) Apoptotic mechanisms in mutant LRRK2-mediated cell death. *Hum. Mol. Genet. 16*, 1319–1326.
15. Greggio, E., Jain, S., Kingsbury, A., Bandopadhyay, R., Lewis, P., Kaganovich, A., van der Brug, M. P., Beilina, A., Blackinton, J., Thomas, K. J., Ahmad, R., Miller, D. W., Kesavapany, S., Singleton, A., Lees, A., Harvey, R. J., Harvey, K., and Cookson, M. R. (2006) Kinase activity is required for the toxic effects of mutant LRRK2/dardarin. *Neurobiol. Dis. 23*, 329–341.
16. Lin, X., Parisiadou, L., Gu, X. L., Wang, L., Shim, H., Sun, L., Xie, C., Long, C. X., Yang, W. J., Ding, J., Chen, Z. Z., Gallant, P. E., Tao-Cheng, J. H., Rudow, G., Troncoso, J. C., Liu, Z., Li, Z., and Cai, H. (2009) Leucine-rich repeat kinase 2 regulates the progression of neuropathology induced by Parkinson's-disease-related mutant α-synuclein. *Neuron 64*, 807–827.
17. West, A. B., Moore, D. J., Choi, C., Andrabi, S. A., Li, X., Dikeman, D., Biskup, S., Zhang, Z., Lim, K. L., Dawson, V. L., and Dawson, T. M. (2007) Parkinson's disease-associated mutations in LRRK2 link enhanced GTP-binding and kinase activities to neuronal toxicity. *Hum. Mol. Genet. 16*, 223–232.
18. Anand, V. S., Reichling, L. J., Lipinski, K., Stochaj, W., Duan, W., Kelleher, K., Pungaliya, P., Brown, E. L., Reinhart, P. H., Somberg, R., Hirst, W. D., Riddle, S. M., and Braithwaite, S. P. (2009) Investigation of leucine-rich repeat kinase 2: Enzymological properties and novel assays. *FEBS J. 276*, 466–478.
19. Luzon-Toro, B., de la Torre, E. R., Delgado, A., Perez-Tur, J., and Hilfiker, S. (2007) Mechanistic insight into the dominant mode of the Parkinson's disease-associated G2019S LRRK2 mutation. *Hum. Mol. Genet. 16*, 2031–2039.
20. Gloeckner, C. J., Schumacher, A., Boldt, K., and Ueffing, M. (2009) The Parkinson disease-associated protein kinase LRRK2 exhibits MAPKKK activity and phosphorylates MKK3/6 and MKK4/7, in vitro. *J. Neurochem. 109*, 959–968.
21. Biskup, S., Moore, D. J., Celsi, F., Higashi, S., West, A. B., Andrabi, S. A., Kurkinen, K., Yu, S. W., Savitt, J. M., Waldvogel, H. J., Faull, R. L., Emson, P. C., Torp, R., Ottersen, O. P., Dawson, T. M., and Dawson, V. L. (2006) Localization of LRRK2 to membranous and vesicular structures in mammalian brain. *Ann. Neurol. 60*, 557–569.
22. Hatano, T., Kubo, S., Imai, S., Maeda, M., Ishikawa, K., Mizuno, Y., and Hattori, N. (2007) Leucine-rich repeat kinase 2 associates with lipid rafts. *Hum. Mol. Genet. 16*, 678–690.
23. MacLeod, D., Dowman, J., Hammond, R., Leete, T., Inoue, K., and Abeliovich, A. (2006) The familial Parkinsonism gene LRRK2 regulates neurite process morphology. *Neuron 52*, 587–593.
24. Plowey, E. D., Cherra, S. J., Liu, Y. J., and Chu, C. T. (2008) Role of autophagy in G2019S-LRRK2-associated neurite shortening in differentiated SH-SY5Y cells. *J. Neurochem. 105*, 1048–1056.
25. Shin, N., Jeong, H., Kwon, J., Heo, H. Y., Kwon, J. J., Yun, H. J., Kim, C. H., Han, B. S., Tong, Y., Shen, J., Hatano, T., Hattori, N., Kim, K. S., Chang, S., and Seol, W. (2008) LRRK2 regulates synaptic vesicle endocytosis. *Exp. Cell Res. 314*, 2055–2065.
26. Alegre-Abarrategui, J., Christian, H., Lufino, M., Mutihac, R., Lourenco Venda, L., Ansorge, O., and Wade-Martins, R. (2009) LRRK2 regulates autophagic activity and localises to specific membrane microdomains in a novel human genomic reporter cellular model. *Hum. Mol. Genet 18*, 4022–4034.
27. Sancho, R. M., Law, B. M., and Harvey, K. (2009) Mutations in the LRRK2 Roc-COR tandem domain link Parkinson's disease to Wnt signalling pathways. *Hum. Mol. Genet 18*, 3955–3968.
28. Greggio, E., Zambrano, I., Kaganovich, A., Beilina, A., Taymans, J. M., Daniels, V., Lewis, P., Jain, S., Ding, J., Syed, A., Thomas, K. J., Baekelandt, V., and Cookson, M. R. (2008) The Parkinson disease-associated leucine-rich repeat kinase 2 (LRRK2) is a dimer that undergoes intramolecular autophosphorylation. *J. Biol. Chem. 283*, 16906–16914.
29. Gloeckner, C. J., Kinkl, N., Schumacher, A., Braun, R. J., O'Neill, E., Meitinger, T., Kolch, W., Prokisch, H., and Ueffing, M. (2006) The Parkinson disease causing LRRK2 mutation I2020T is associated with increased kinase activity. *Hum. Mol. Genet. 15*, 223–232.
30. Klein, C. L., Rovelli, G., Springer, W., Schall, C., Gasser, T., and Kahle, P. J. (2009) Homo- and heterodimerization of ROCO kinases: LRRK2 kinase inhibition by the LRRK2 ROCO fragment. *J. Neurochem. 111*, 703–715.
31. Deng, J., Lewis, P. A., Greggio, E., Sluch, E., Beilina, A., and Cookson, M. R. (2008) Structure of the ROC domain from the Parkinson's disease-associated leucine-rich repeat kinase 2 reveals a dimeric GTPase. *Proc. Natl. Acad. Sci. U.S.A. 105*, 1499–1504.
32. LaVoie, M. J., Ostaszewski, B. L., Weihofen, A., Schlossmacher, M. G., and Selkoe, D. J. (2005) Dopamine covalently modifies and functionally inactivates parkin. *Nat. Med. 11*, 1214–1221.
33. Li, X., Tan, Y. C., Poulose, S., Olanow, C. W., Huang, X. Y., and Yue, Z. (2007) Leucine-rich repeat kinase 2 (LRRK2)/PARK8 possesses GTPase activity that is altered in familial Parkinson's disease R1441C/G mutants. *J. Neurochem. 103*, 238–247.
34. Greggio, E., Lewis, P. A., van der Brug, M. P., Ahmad, R., Kaganovich, A., Ding, J., Beilina, A., Baker, A. K., and Cookson, M. R. (2007) Mutations in LRRK2/dardarin associated with Parkinson disease are more toxic than equivalent mutations in the homologous kinase LRRK1. *J. Neurochem. 102*, 93–102.
35. Korr, D., Toschi, L., Donner, P., Pohlenz, H. D., Kreft, B., and Weiss, B. (2006) LRRK1 protein kinase activity is stimulated upon binding of GTP to its Roc domain. *Cell. Signalling 18*, 910–920.
36. Ruxton, G. D. (2006) The unequal variance t-test is an underused alternative to Student's t-test and the Mann-Whitney U-test. *Behav. Ecol. 17*, 688–690.
37. Picton, C., Klee, C. B., and Cohen, P. (1980) Phosphorylase kinase from rabbit skeletal muscle: Identification of the calmodulin-binding subunits. *Eur. J. Biochem. 111*, 553–561.

38. LaVoie, M. J., Fraering, P. C., Ostaszewski, B. L., Ye, W., Kimberly, W. T., Wolfe, M. S., and Selkoe, D. J. (2003) Assembly of the γ-secretase complex involves early formation of an intermediate subcomplex of Aph-1 and nicastrin. *J. Biol. Chem. 278*, 37213–37222.
39. Osenkowski, P., Li, H., Ye, W., Li, D., Aeschbach, L., Fraering, P. C., Wolfe, M. S., and Selkoe, D. J. (2009) Cryoelectron microscopy structure of purified γ-secretase at 12 Å resolution. *J. Mol. Biol. 385*, 642–652.
40. Gu, Y., Sanjo, N., Chen, F., Hasegawa, H., Petit, A., Ruan, X., Li, W., Shier, C., Kawarai, T., Schmitt-Ulms, G., Westaway, D., St George-Hyslop, P., and Fraser, P. E. (2004) The presenilin proteins are components of multiple membrane-bound complexes that have different biological activities. *J. Biol. Chem. 279*, 31329–31336.
41. Kimberly, W. T., LaVoie, M. J., Ostaszewski, B. L., Ye, W., Wolfe, M. S., and Selkoe, D. J. (2002) Complex N-linked glycosylated nicastrin associates with active γ-secretase and undergoes tight cellular regulation. *J. Biol. Chem. 277*, 35113–35117.
42. Kimberly, W. T., LaVoie, M. J., Ostaszewski, B. L., Ye, W., Wolfe, M. S., and Selkoe, D. J. (2003) γ-Secretase is a membrane protein complex comprised of presenilin, nicastrin, Aph-1, and Pen-2. *Proc. Natl. Acad. Sci. U.S.A. 100*, 6382–6387.
43. Janssen, R. J., Nijtmans, L. G., van den Heuvel, L. P., and Smeitink, J. A. (2006) Mitochondrial complex I: Structure, function and pathology. *J. Inherited Metab. Dis. 29*, 499–515.
44. Sen, S., Webber, P. J., and West, A. B. (2009) Dependence of leucine-rich repeat kinase 2 (LRRK2) kinase activity on dimerization. *J. Biol. Chem. 284*, 36346–36356.
45. Klein, C. L., Rovelli, G., Springer, W., Schall, C., Gasser, T., and Kahle, P. J. (2009) Homo- and heterodimerization of ROCO kinases: LRRK2 kinase inhibition by the LRRK2 ROCO fragment. *J. Neurochem. 111*, 703–715.
46. Jorgensen, N. D., Peng, Y., Ho, C. C., Rideout, H. J., Petrey, D., Liu, P., and Dauer, W. T. (2009) The WD40 domain is required for LRRK2 neurotoxicity. *PLoS One 4*, e8463.
47. Lewis, P. A., Greggio, E., Beilina, A., Jain, S., Baker, A., and Cookson, M. R. (2007) The R1441C mutation of LRRK2 disrupts GTP hydrolysis. *Biochem. Biophys. Res. Commun. 357*, 668–671.
48. Ito, G., Okai, T., Fujino, G., Takeda, K., Ichijo, H., Katada, T., and Iwatsubo, T. (2007) GTP binding is essential to the protein kinase activity of LRRK2, a causative gene product for familial Parkinson's disease. *Biochemistry 46*, 1380–1388.
49. Guo, L., Gandhi, P. N., Wang, W., Petersen, R. B., Wilson-Delfosse, A. L., and Chen, S. G. (2007) The Parkinson's disease-associated protein, leucine-rich repeat kinase 2 (LRRK2), is an authentic GTPase that stimulates kinase activity. *Exp. Cell Res. 313*, 3658–3670.
50. Gallo, K. A., and Johnson, G. L. (2002) Mixed-lineage kinase control of JNK and p38 MAPK pathways. *Nat. Rev. Mol. Cell Biol. 3*, 663–672.
51. Ramos, J. W. (2008) The regulation of extracellular signal-regulated kinase (ERK) in mammalian cells. *Int. J. Biochem. Cell Biol. 40*, 2707–2719.
52. Kyriakis, J. M., and Avruch, J. (2001) Mammalian mitogen-activated protein kinase signal transduction pathways activated by stress and inflammation. *Physiol. Rev. 81*, 807–869.
53. Greggio, E., Taymans, J. M., Zhen, E. Y., Ryder, J., Vancraenenbroeck, R., Beilina, A., Sun, P., Deng, J., Jaffe, H., Baekelandt, V., Merchant, K., and Cookson, M. R. (2009) The Parkinson's disease kinase LRRK2 autophosphorylates its GTPase domain at multiple sites. *Biochem. Biophys. Res. Commun. 389*, 449–454.
54. Kamikawaji, S., Ito, G., and Iwatsubo, T. (2009) Identification of the autophosphorylation sites of LRRK2. *Biochemistry 48*, 10963–10975.
55. Goodman, T., Schulenberg, B., Steinberg, T. H., and Patton, W. F. (2004) Detection of phosphoproteins on electroblot membranes using a small-molecule organic fluorophore. *Electrophoresis 25*, 2533–2538.
56. Liu, M., Dobson, B., Glicksman, M. A., Yue, Z., and Stein, R. L. (2010) Kinetic mechanistic studies of wild-type leucine-rich repeat kinase 2: Characterization of the kinase and GTPase activities. *Biochemistry 49*, 2008–2017.
57. Lovitt, B., Vanderporten, E. C., Sheng, Z., Zhu, H., Drummond, J., and Liu, Y. (2010) Differential effects of divalent manganese and magnesium on the kinase activity of leucine-rich repeat kinase 2 (LRRK2). *Biochemistry 49*, 3092–3100.
58. Nichols, R. J., Dzamko, N., Hutti, J. E., Cantley, L. C., Deak, M., Moran, J., Bamborough, P., Reith, A. D., and Alessi, D. R. (2009) Substrate specificity and inhibitors of LRRK2, a protein kinase mutated in Parkinson's disease. *Biochem. J. 424*, 47–60.
59. Blom, N., Gammeltoft, S., and Brunak, S. (1999) Sequence and structure-based prediction of eukaryotic protein phosphorylation sites. *J. Mol. Biol. 294*, 1351–1362.
60. Liou, A. K., Leak, R. K., Li, L., and Zigmond, M. J. (2008) Wild-type LRRK2 but not its mutant attenuates stress-induced cell death via ERK pathway. *Neurobiol. Dis. 32*, 116–124.
61. Raman, M., Chen, W., and Cobb, M. H. (2007) Differential regulation and properties of MAPKs. *Oncogene 26*, 3100–3112.